Reprinted from Vol. 78—Low Light Level Devices

PHOTOELECTRON MICROSCOPY OF BIOLOGICAL SURFACES. EXCITATION SOURCE BRIGHTNESS REQUIREMENTS

Rudy J. Dam and O. Hayes Griffith
Institute of Molecular Biology and Department of Chemistry,
University of Oregon, Eugene, Oregon 97403

Abstract

Photoelectron microscopy is a surface technique which provides topographical information using the photoelectric effect as a basis for contrast. Progress in the biological applications of this technique is briefly reviewed. Due to relatively low quantum yields, photoemission from biological samples is weak and an image intensifier is used in order to visualize and record the photoelectron image. Currently the limiting magnification is determined by UV power incident on the sample. Power requirements for high-magnification imaging are calculated in terms of microscope, sample, and image intensifier parameters. To approach 40 Å resolution, an instrument magnification of 12,000-50,000 is required along with a UV intensity of 0.01 to 10 Watts/cm^2 depending on the wavelength and sample. For a tightly focused laser source the total power requirement is 1 mWatt or less.

Introduction

Determining the topography of biological surfaces is a challenging problem because of the enormous microheterogeneity in the various proteins, lipids and saccharides present. The photoelectric effect has the potential of mapping the distributions of specific cell surface components without interference from the cellular contents. The basic idea of photoelectron microscopy (PEM) is illustrated in Figure 1. The sample is placed in a vacuum system and subjected to UV light. As the UV source is scanned to shorter wavelengths the surface molecules with the lowest ionization potentials will begin to photoeject electrons which are then accelerated, passed through a series of electron lenses and imaged onto a phosphor screen. This is a very different approach from fluorescence microscopy or transmission or scanning electron microscopy, as shown in Figure 2. There is no electron gun in PEM, the sample is the source of electrons. Indeed, it is a very weak electron source, requiring the use of image intensifiers at even moderate magnifications.

The origin of photoelectron microscopy dates back to the early days of electron microscopy when emission microscopes were constructed to examine hot filaments for use in early transmission microscopes, oscilliscopes and television tubes. Biological surface studies are a relatively new development. The first photoelectron images of mammalian [1] and plant [2] samples are shown in Figures 3 and 4. These are very preliminary low magnification images. Several additional reports examine specific aspects of PEM applications to organic and biological surfaces [3-10]. Metallurgical applications are reviewed elsewhere [11]. Our aim here is to provide a brief overview of the technique and to discuss in detail the UV power requirements for high resolution photoelectron microscopy experiments.

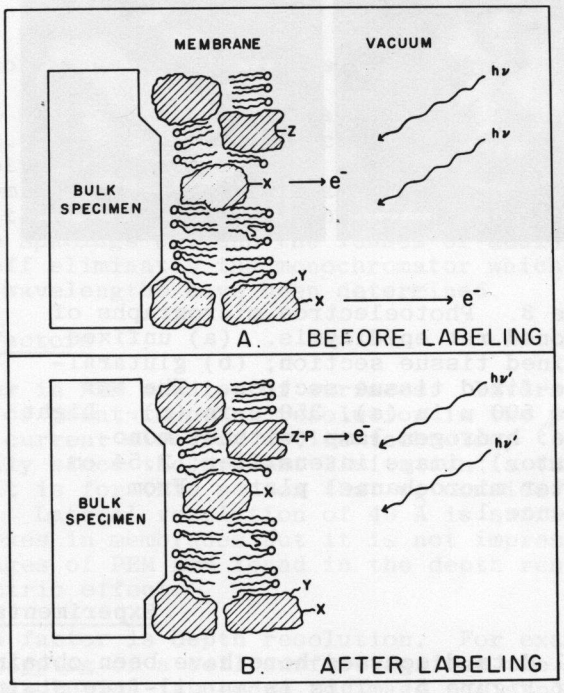

Figure 1. Photoionization of electrons from a hypothetical biological surface. The top diagram illustrates intrinsic photoionization from certain functional groups (X) on the surface. In the bottom diagram, the site Z has been labeled with a photoelectron label P and the energy of the incident light has been lowered from hν to hν', below the ionization threshold of X. Photoelectrons then originate predominantly from sites Z-P. From reference 1.

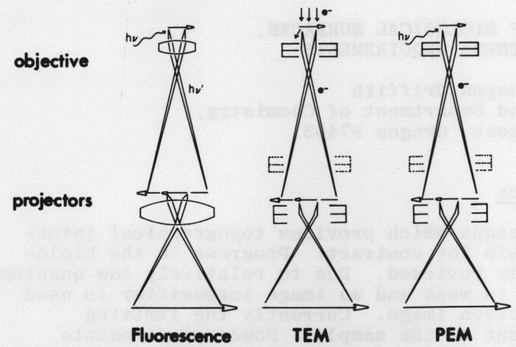

Figure 2. The techniques of fluorescence microscopy, TEM and PEM compared. PEM shares with fluorescence the use of incident exciting light, and with TEM the advantages of electron image formation. From reference 2.

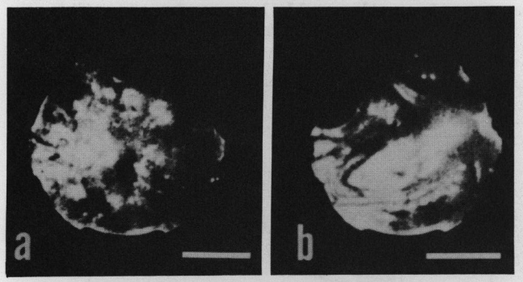

Figure 3. Photoelectron micrographs of sectioned rat epididymis. (a) unfixed unstained tissue section; (b) glutaraldehyde-fixed tissue section. The bar equals 500 μ in (a), 350 μ in (b). Light source: hydrogen lamp (without monochromator); image intensifier: 2.54 cm diameter microchannel plate. From reference 1.

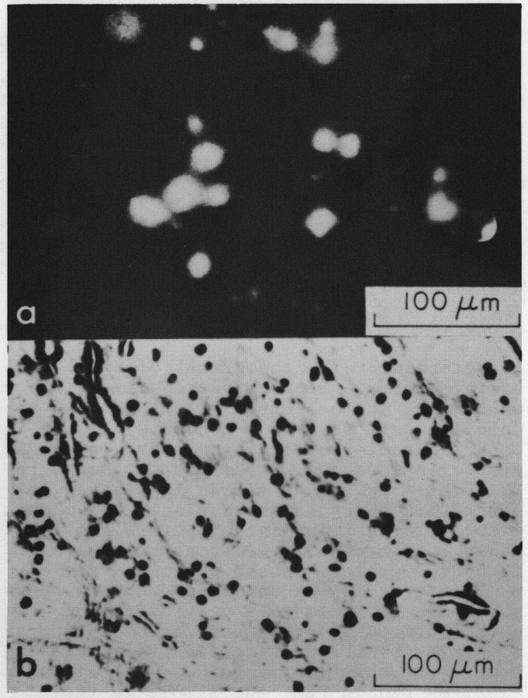

Figure 4. (a) Photoelectron micrograph of a freeze-cleaved chloroplast preparation. Light source: hydrogen lamp, with monochromator set for 200 ± 10 nm. Image intensifier: 4 cm, three-stage electrostatic. (b) Reflected light micrograph of the same sample (but not the same field of view). The chloroplasts are visible as small black spots against a bright field. From reference 2.

Experimental Apparatus

All data discussed here have been obtained on the prototype photoelectron microscope (a) of Figure 5. This is an oil-free stainless steel ultrahigh vacuum chamber with Varian Conflat copper-sealing flanges and an ion pump to minimize contamination of the sample surface. The two electron lenses are of the electrostatic unipotential type and were designed for very low magnifications (x10 - 200) so that very faint images can be observed, even with a conventional hydrogen discharge lamp-monochromator combination. In Figure 5(a) the monochromatic light is reflected from a magnesium fluoride coated aluminum mirror, through the objective lens, and onto the sample. The light arrives very nearly normal to the sample surface, which is useful in studying the effects of polarization, substrate reflection and optical interference. The sample is at -10kV so that the photoejected electrons are accelerated toward the anode, focused, and passed through a small hole in the mirror, projector lens and onto a microchannel plate image intensifier and phosphor screen. Subsequently the microchannel plate has been replaced by an external 40 mm 3-stage Varo Inc. electrostatic image intensifier coupled to an aluminized phosphor-coated fiber optics window. The aluminized layer

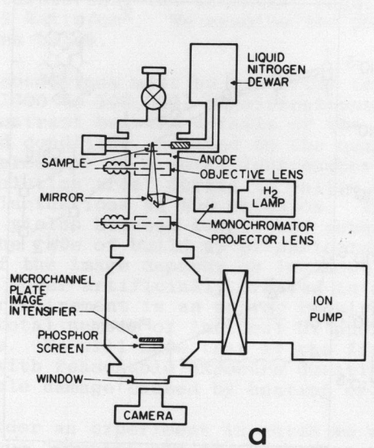

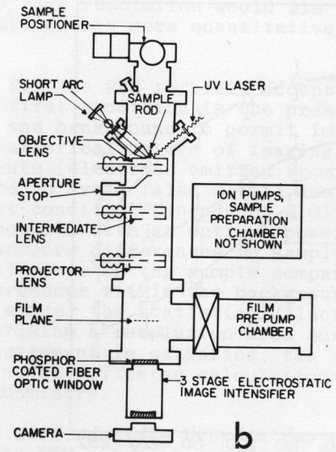

Figure 5. Schematic diagrams of the photoelectron microscope. (a) Prototype low-magnification instrument. (b) High-magnification instrument nearing completion. The major design improvements include a more efficient UV optical geometry with provision for laser excitation, addition of an intermediate electron lens, aperture stop, provision for an internal camera system, and ultrahigh vacuum sample preparation chamber.

reduces the stray UV light reaching the phosphor-image intensifier system.

Figure 5(b) shows the essential features of a second ultrahigh vacuum PEM currently nearing completion at the University of Oregon. The sample may be cooled to 77°K in order to study frozen samples, as in the prototype microscope. The design of the new instrument emphasizes high light intensity from either a conventional UV source (12) or a laser (13), and higher magnification (initially x10,000). Much higher magnifications can be obtained simply by increasing the spacings between the lenses or adding an additional projector lens. The design trade off eliminates the monochromator which is no longer needed after the optimal excitation wavelengths have been determined.

Resolution Factors

There are two resolution factors to consider in PEM studies of surfaces: lateral resolution and depth resolution. The lateral or point-to-point resolution in the plane of the sample is estimated to be 25-40 Å with current electron optics technology (1). However, this has not been tested experimentally since the present limitation is the light source-image intensifier combination. It is for this reason that we consider the light source requirements in detail below. Lateral resolution of 40 Å is sufficient to map the distribution of many protein complexes in membranes but it is not impressive by electron microscopy standards. The advantages of PEM are found in the depth resolution and contrast inherent in the photoelectric effect.

The second and equally important resolution factor is depth resolution. For example, a depth resolution of 100 Å would permit the mapping of a cell surface against the background of the cytoplasm whereas a higher resolution is needed to image the exposed half of the 80-100 Å thick membrane without interference from the inner half of the membrane. More quantitatively, exponential curve fitting of image brightness data vs. sample thickness defines a characteristic depth resolution factor, d_o, from which approximately 60% (i.e., $1-e^{-1}$) of the electrons originate. For the model compound phthalocyanine, d_o = 15 Å ± 5 Å (4,14). This is perhaps the highest known depth resolution factor of any microscopic technique. It is a direct result of the very low kinetic energy and hence short escape depth of the photoelectrons.

Contrast

Every molecule has a characteristic set of ionization potentials that contribute to a photoelectron quantum yield curve. There is very little literature on the electron

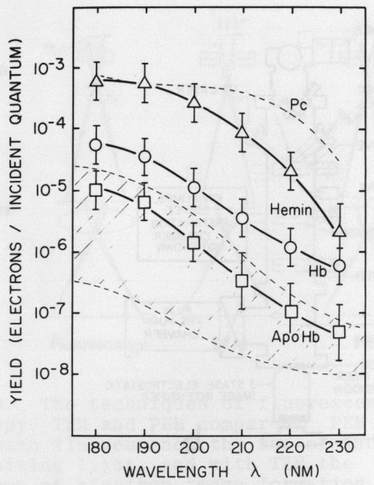

Figure 6. Photoelectron quantum yield curves for hemin, hemoglobin and apohemoblobin (ApoHb). The dashed curve (P_c) is the yield of phthalocyanine reported by Schechtman (15). The shaded band contains the quantum yield data for the amino acids. From reference 7.

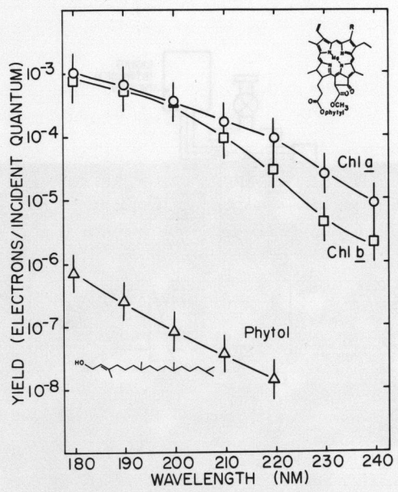

Figure 7. Photoelectron quantum yield curves for chlorophyll a ($R = CH_3$, circles), chlorophyll b ($R = CHO$, squares) and phytol (triangles). From reference 8.

quantum yields of biological macromolecules. Some representative data are shown in Figures 6 and 7. The photoelectron quantum yields of 19 amino acids fall within the shaded area of Figure 6 (only the aromatic amino acids L-tryptophan and L-tyrosine rise slightly above this band at short wavelengths). Since proteins are composed of amino acids and the yields appear to be additive, the curves for all proteins without prosthetic groups should lie within this band. Apohemoglobin does fall within this band as predicted. Hemin (ferriheme chloride) has a photoelectron quantum yield curve two orders of magnitude larger. The curve for the intact hemoglobin molecule (apohemoglobin + heme) is intermediate and can be estimated from the previous two quantum yield curves assuming a simple dilution model (7). It may prove possible to map the positions for the heme proteins such as the cytochromes using the heme as an intrinsic photoelectron label.

Figure 7 shows the quantum yield curves of the chlorophylls a and b. These curves lie three orders of magnitude above that of the long phytol tail showing that the photoelectric effect is due almost entirely to the porphyrin head group. The quantum yield curves of the chlorophylls are clearly much greater than those of the protein and lipids, so that at high resolution photoelectron microscopy will be useful in mapping chlorophyll distributions in photosynthetic membranes. Chlorophyll is not readily visualized by conventional electron microscopy because the elemental composition and hence electron scattering does not differ greatly from the naturally occurring cell surface components. There are many other photoemissive molecules including phthalocyanine, acridine orange and a carcinogen, benzo(a)pyrine. Tagging antibodies with a photoemissive molecule should permit immunophotoelectric experiments, complimentary to immunofluorescence studies of cell surfaces (1,9).

UV Power Required to Attain 40 Å Resolution

In this section we discuss the UV power requirement problem. A general formula will be derived relating the required UV intensity to a number of microscope and sample variables. Using the best available estimates for their values, we calculate the UV power required to obtain suitable image quality with various sample materials and magnifications. Since the light intensity needed increases as the square of the magnification, attaining 40 Å resolution will require the intensity to increase by a factor of $(50{,}000/100)^2 = 2.5 \times 10^5$ over the x100 prototype instrument. We have roughly estimated the UV intensity in the prototype PEM to be 10^{-6}-10^{-5} Watt/cm^2 at 200 ± 10 nm.

This predicts that the intensity required for high resolution would lie in the range 0.2 to 2 Watts/cm^2. We examine the power requirements more quantitatively in the calculations below.

Two conditions must be satisfied in order for the PEM to yield acceptable images at high (x1000 to 100,000) magnifications. The first condition is the presence of sufficient contrast between details of the sample and background to permit image formation. A second condition, related to the quantum statistical nature of imaging with electrons, is the presence of a sufficient number of events (electrons emitted from the sample) per resolution area* during an entire exposure to avoid false detail due to statistical fluctuations in the emission. The first condition depends on a difference in quantum yields between sample and substrate coupled with an optical power requirement, since the rate of build up of photographic exposure differences in sample and background areas of the image depends on incident optical power on the sample compared to the "noise" power artificially created in the microscope within the background areas. The second requirement is an energy requirement, since the statistical fluctuations depend on the total number of incident UV photons striking a resolution area during a complete exposure. We will show that if the first requirement is satisfied, the second can be met with reasonable exposure durations. In the following calculations, we neglect any sample damage caused by heating or photochemistry.

Consider an experiment in which we wish to differentiate between two adjacent surfaces, the "sample" and the "substrate", in the PEM. Let the incident UV flux density be P photons cm^{-2} sec^{-1} of wavelength λ. We define quantum yields (electrons emitted/incident photon) of the sample and substrate to be $Y_s(\lambda)$ and $Y_b(\lambda)$ respectively. The photoelectrons are accelerated to 25 kV and travel down the length of the PEM. They strike a phosphor screen, typically producing 200 photons of green light per incident electron. This light passes through a fiber optic window and is amplified by the three-stage image intensifier with a gain of $\sim 5 \times 10^4$. The resulting image brightness can be either photographed or measured quantitatively using a photomultiplier tube (see Figure 5).

To characterize the experiment completely will require the following additional definitions,

$N_s \equiv$ sample electron emission density, electrons cm^{-2}sec^{-1} leaving sample

$N_b \equiv$ substrate electron emission density

$\gamma \equiv$ photoelectron transport efficiency = fraction of photoelectrons that reach the phosphor screen

$G \equiv$ total gain of phosphor-image intensifier system = (no. of photons leaving output stage of intensifier)/(no. of photoelectrons reaching first phosphor)

$B_s \equiv$ final image flux density of sample in photons cm^{-2}sec^{-1}

$B_b \equiv$ final image flux density of substrate

$B_v \equiv$ image flux density due to intrinsic image intensifier noise (assumed constant)

$M \equiv$ linear magnification of microscope

The imaging system is schematically shown in Figure 8. From this point on we drop the explicit wavelength dependence in our expressions.

Since $N_s = PY_s$ and $N_b = PY_b$, we have

$$B_s = \frac{N_s \gamma G}{M^2} = \frac{PY_s \gamma G}{M^2} \text{ photons cm}^{-2}\text{sec}^{-1} \quad (1)$$

$$B_b = \frac{N_b \gamma G}{M^2} = \frac{PY_b \gamma G}{M^2} \text{ photons cm}^{-2}\text{sec}^{-1} \quad (2)$$

* "Resolution area" is the area associated with a resolved point image. It is given approximately by r^2 if the lateral point-to-point resolution is r.

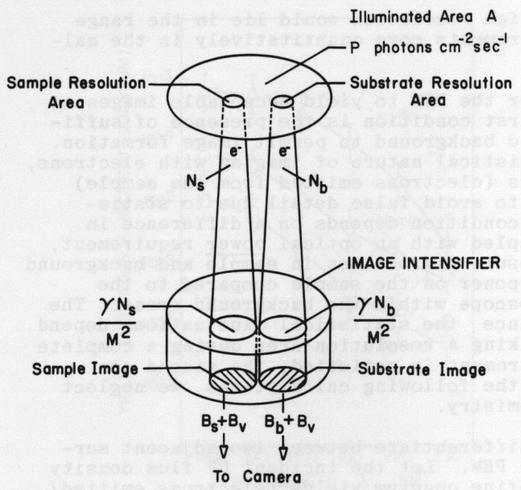

Figure 8. Schematic diagram of the photoelectron microscope-image intensifier system used in the power requirement calculations.

The actual brightness of the sample and substrate images will be $(B_S + B_V)$ and $(B_b + B_V)$ respectively. In order to distinguish between them (e.g., on a photographic plate) the following must be met:

$$(B_s + B_v) \geq K(B_b + B_v)$$

where K is an empirically determined constant chosen to provide adequate contrast. We can rewrite this equation in the form

$$B_s \geq KB_b + (K-1)B_v \tag{3}$$

Substituting Eqs. (1) and (2) into (3) and rearranging,

$$\frac{P\gamma G}{M^2}\left(Y_s - KY_b - (K-1)B_v\left(\frac{M^2}{P\gamma G}\right)\right) \geq 0 \tag{4}$$

The first factor is always ≥ 0. Therefore in order for the inequality to hold we must have

$$Y_s - KY_b \geq (K-1)B_v\left(\frac{M^2}{P\gamma G}\right) \tag{5}$$

Solving for P gives the final result:

$$P \geq \frac{(K-1)B_v M^2}{(Y_s - KY_b)\gamma G} \text{ photons cm}^{-2}\text{sec}^{-1} \tag{6}$$

We note that when $Y_S \to KY_b$ the intensity requirement becomes arbitrarily large. This simply reflects the fact that no contrast is possible at any power level when the quantum yield of the sample becomes too small, i.e., on the order of KY_b.

Eq. (6) can be manipulated to eliminate the parameters γ and G, so that P depends only on the instrument parameters M, B_V, and K, and the parameters Y_S and Y_b, as follows. We imagine the microscope operating at a given magnification M_O with no input light on the sample. In this condition the intensifier optical output is B_V, due to noise. We can attribute this B_V to a fictitious electron emission density at the sample, N_V^O electrons $cm^{-2}sec^{-1}$, in the absence of light. The relation between B_V and N_V^O is therefore

$$B_v = \frac{\gamma G N_v^O}{M_o^2} \tag{7}$$

If we can determine N_V^O, we can insert (7) into (6) to obtain the value of P at any M.

$$P \geq \frac{(K-1)N_v^O}{Y_s - KY_b}\left(\frac{M}{M_o}\right)^2 \tag{8}$$

We note that for B_V to be independent of magnification in this model we must have N_V^O varying with M_O such that

$$\left(\frac{N_v^O}{M_o^2}\right) = \text{const.} \equiv N_v' \tag{9}$$

N_V' is thus a more useful "noise constant" for use in Eq. (8) which becomes

$$P \geq \frac{(K-1)N_v' M^2}{Y_s - KY_b} \tag{10}$$

By measuring values of B_S for the case $B_S >> B_V$ with a homogeneous sample and various neutral density filters between the UV source and the sample, we have determined that the imaging system is linear over a three decade range [4]. Then by noting the degree of film darkening corresponding to various input levels when B_S is recorded photographically, we have determined that a one-decade change in B_S gives an appreciable change in film density. Thus K = 10 appears to be a reasonable choice for good image contrast in photomicrography; it may well be an overestimate.

The quantity N_V' was measured as follows. We attached a phototube to the three stage image intensifier and irradiated a homogeneous sample of dye molecules (copper phthalocyanine, with a moderately high Y_S) so as to produce an output brightness $B_S + B_V \approx B_S$. A magnification M_O of 60 was used. The phototube output current I_S was measured as well as the current between the sample and ground in the PEM. The PEM current was 6×10^{-12} amperes and the total sample area was 0.12 cm^2; thus the actual electron emission density at the sample was

$$N_s^O = 3.13 \times 10^8 \text{ electrons cm}^{-2}\text{sec}^{-1} \tag{11}$$

With the UV light off the phototube current I_V was measured, corresponding to the PEM optical noise. Since the system is linear,

$$\frac{I_v}{I_s} = \frac{B_v}{B_s} = \frac{\gamma G N_v^O M_o^2}{\gamma G N_s^O M_o^2} = \frac{N_v^O}{N_s^O} \tag{12}$$

In our experiment $I_V/I_S = 1.28 \times 10^{-2}$, hence $N_V^O = 4.0 \times 10^6$ electrons $cm^{-2}sec^{-1}$ from Eqs. (11) and (12). Finally, since M_O=60 in this experiment, we obtain from Eq. (9)

$$N_v' = \frac{4 \times 10^6}{(60)^2} = 1.11 \times 10^3 \text{ electrons cm}^{-2}\text{sec}^{-1} \tag{13}$$

We are now able to calculate the minimum photon flux using Eq. (10). To describe the input optical quantities in conventional physical units, we note that each photon carries an energy $h\nu = hc/\lambda = 1.986 \times 10^{-25} \times \lambda^{-1}$ joules, where λ is in meters. If we further assume an illuminated area A on the sample, the input power in Watts at the wavelength λ is

$$W \geq \frac{hcA(K-1)N_v' M^2}{(Y_s - KY_b)\lambda} = \frac{2.0 \times 10^{-21}\, AM^2}{(Y_s - 10Y_b)\lambda} \tag{14}$$

with A measured in cm^2 and λ in meters.

Results of the UV Power Requirements Calculation

We have used Eq. (14) along with results of quantum yield measurements for samples and substrate to calculate estimates of the minimum W for an illuminated area of 0.05 cm^2 (corresponding to an image of a 2.5 mm diameter arc source) and an illuminated area of 10^{-6} cm^2 (attainable with lasers). Table 1 presents the quantum yield values for a Formvar substrate and for two samples, phthalocyanine and poly-L-tryptophan. Entries in Tables 2-4 are milliwatts of average power that will produce minimum acceptable photoelectron images of the samples listed, according to Eq. (14).

Table 1. The absolute electron quantum yield per incident photon for Formvar (Y_b), phthalocyanine, and poly-L-tryptophan as a function of wavelength λ.

λ(nm)	$Y_b(\lambda)$	$Y_s(\lambda)$, phthalocyanine	$Y_s(\lambda)$, poly-L-tryptophan
230	$<< 10^{-7}$	3.8×10^{-5}	2×10^{-7}
210	$<< 10^{-7}$	4.0×10^{-4}	2×10^{-6}
190	1.5×10^{-6}	5.2×10^{-4}	6×10^{-5}

The intensity (photons $cm^{-2}sec^{-1}$) available at the sample is a factor of $.05/10^{-6} = 5 \times 10^4$ higher for a laser than for an arc source of comparable power (the actual ratio may be even larger depending on the efficiency of the optical system used to image the arc). Laser sources in the 180-220 nm region are very promising for this application since the average power required in a tightly focused laser system is quite modest. Consider for example the power requirements in Table 2 for metal-free phthalocyanine. This compound is a very strong photoemitter at all wavelengths shorter than 230 nm and it is used as a standard in our quantum yield measurements. It does not represent the typical case we expect to encounter. Nevertheless, the calculations predict that only 10^{-4} - 10^{-3} milliwatts of incident light (per 100 μ^2 sample area) would be required to observe the image of a cluster of phthalocyanine molecules at x100,000. The polyamino acids of Tables 3 and 4 require higher powers, but still on the order of or less than one milliwatt.

Table 2. Milliwatts of incident light required to view metal-free phthalocyanine using an arc source (A=.05 cm^2) and a laser (A=$10^{-6}cm^2$).

			Instrument Magnification, M			
λ(nm)	Y_s-10Y_b	A,cm^2	100,000	50,000	10,000	1,000
230	3.8×10^{-5}	.05	114	29	1.14	11×10^{-3}
210	4.0×10^{-4}	.05	12	3	0.12	1.2×10^{-3}
190	5.1×10^{-4}	.05	10	2.6	0.10	1.0×10^{-3}
230	3.8×10^{-5}	10^{-6}	23×10^{-4}	57×10^{-5}	23×10^{-6}	23×10^{-8}
210	4.0×10^{-4}	10^{-6}	2.4×10^{-4}	6.0×10^{-5}	2.4×10^{-6}	2.4×10^{-8}
190	5.1×10^{-4}	10^{-6}	2.1×10^{-4}	5.2×10^{-5}	2.1×10^{-6}	2.1×10^{-8}

Table 3. Milliwatts of incident light required to view poly-L-tryptophan.

			Instrument Magnification, M			
λ	Y_s-10Y_b	A,cm^2	100,000	50,000	10,000	1,000
230	2×10^{-7}	.05	2.2×10^{4}	5.4×10^{3}	2.2×10^{2}	2.2
210	2×10^{-6}	.05	2.4×10^{3}	6.0×10^{2}	24	.24
190	4.5×10^{-5}	.05	1.2×10^{2}	29	1.2	1.2×10^{-2}
230	2×10^{-7}	10^{-6}	0.43	0.11	4.3×10^{-3}	4.3×10^{-5}
210	2×10^{-6}	10^{-6}	4.8×10^{-2}	1.2×10^{-2}	4.8×10^{-4}	4.8×10^{-6}
190	4.5×10^{-5}	10^{-6}	2.3×10^{-3}	5.9×10^{-4}	2.3×10^{-5}	2.3×10^{-7}

Table 4. Milliwatts of incident light required to view poly-L-arginine HCl. The value of (Y_s-10Y_b) is quite uncertain and was here taken to be 0.1×10^{-5}.

			Instrument Magnification, M			
λ	Y_s-10Y_b	A,cm^2	100,000	50,000	10,000	1,000
180	1×10^{-6}	.05	5.6×10^{3}	1.4×10^{3}	56	0.56
180	1×10^{-6}	10^{-6}	0.11	2.8×10^{-2}	1.1×10^{-3}	1.1×10^{-5}

The absence of entries in Table 4 for wavelengths other than 180 nm reflects the fact that the quantum yield of this polymer is on the order of or less than 10 Y_b for a Formvar substrate. Thus, at wavelengths longer than 180 nm, little or no contrast would be possible regardless of input power. This is fortunate. The preliminary data suggest that many polypeptides and other possible surface components will contribute minimal background signals, which means higher contrast in photoelectron labeling experiments. (The analogy in fluorescence microscopy is a low intrinsic fluorescence.)

Having established the UV power levels required for high-magnification work, we now consider the relationship between magnification and resolution.

The Dependence of Resolution on Magnification

The limiting resolution of an optical system whose separate components have resolution limits r_1, r_2, ... is given by

$$r_{sys} = (r_1^2 + r_2^2 + \ldots)^{\frac{1}{2}} \qquad (15)$$

Consider a two-component system consisting of the PEM and image intensifier. For the purposes of this calculation we take the lateral resolution of the PEM as r_1 = 40 Å. The resolving power of the three-stage image intensifier is 28 lp/mm corresponding to 36 μ at the intensifier output stage. To refer this resolution limit back to the specimen plane in Å we divide by the instrument magnification M (the intensifier magnification is about 1), so that $r_2 = 3.6 \times 10^5/M$ (Å). Thus we obtain for this system

$$r_{sys} = (1600 + 1.3\times10^{11}/M^2)^{\frac{1}{2}} \text{ Å} \qquad (16)$$

The system resolution is limited mainly by the image intensifier at low magnifications (M < 5,000) and by the microscope at high magnifications (M > 20,000). At intermediate M both components contribute significantly to r_{sys}.

Further magnification is often required to visualize r_{sys} on the final micrograph. In most cases the image on the intensifier output will be photographed through a conventional optical system to produce the final negative or print. If m is the photographic magnification introduced by this last step, the image separation between two point objects at the system limit is r_{sys}Mm. In order to be visible to the eye this separation must be of order 100 μ=10^6 Å at a standard viewing distance of 25 cm under optimum conditions. This figure is often increased to 250 μ = 1/4 mm for ease of visibility (16).

Adopting the latter value of 250 μ, we calculate first the minimum M required to achieve a given r_{sys} using Eq. (16) and the subsequent photographic magnification m required to achieve 250 μ separation on the final print. The same final result could also be achieved without photographic enlargement by increasing M. Thus a range of possible M values exists which will provide the required image separation for a given r_{sys}. The following table lists the results of these calculations. The smallest M value in each range corresponds to the solution of Eq. (16) and requires the largest m in order to realize the final print magnification Mm.

Table 5. Magnification required to achieve a given resolution r_{sys}

r_{sys}, Å	range of M	range of m	mM
50	12,000-50,000	4.2-1	50,000
100	3,600-25,000	7-1	25,000
1000	360-2500	7-1	2,500

These calculations show that the limiting resolution of the microscope can be approached using instrument magnifications in the range 12,000 - 50,000 and the incident power levels shown in Tables 2-4.

Statistics of the Photoelectron Image

To evaluate the effect of statistical fluctuations in the electron emission, we consider the number of electrons emitted from a resolution area element r_{sys}^2 during a reasonable exposure time with a given UV power input $P = \beta P_{min} \geq P_{min}$. Recall that

$$P_{min} = \frac{(K-1)N_v'M^2}{Y_s - KY_b} \text{ photons cm}^{-2}\text{sec}^{-1} \qquad (10)$$

Consider an incident power βP_{min}. The sample emission density with this power input is $N_s = \beta P_{min} Y_s$ electrons cm^{-2} sec^{-1}. We follow the electrons through the PEM, image intensifier, and camera system. Assuming no losses in the electron optics, γ = 1 and the photon flux density at the output stage of the image intensifier is

$$F_{int} = B_s + B_v \approx GN_s/M^2 = \frac{\beta G(K-1)N_v'}{1 - KY_b/Y_s} \text{ photons sec}^{-1}\text{cm}^{-2} \qquad (17)$$

The noise contribution term $B_v = GN_v'$ has been neglected since it will be smaller than B_s by at least a factor of $\beta(K-1) \approx 10$. If this image is photographed with an optical system of efficiency ε, the flux density at the film plane will be

$$F_{film} = F_{int}\varepsilon = \frac{\beta\varepsilon G(K-1)N_v'}{1 - KY_b/Y_s} \qquad (18)$$

Optical efficiency here is defined as the photon flux received at the film plane divided by the flux at the output stage of the image intensifier. It can be estimated from the optical parameters of the camera system and the magnification m. If the source radiates uniformly into 2π steradians, ε is of order 10^{-2} for a lens system of focal ratio F/1.2 working near unit magnification.

In order to calculate the exposure time it is convenient to convert photons $sec^{-1}cm^{-2}$ to foot-candles. For λ = 550 nm light the conversion factor is 1 photon $cm^{-2}sec^{-1}$ = 2.26×10^{-13} ft-c (see, e.g., reference 17). Inserting the previously calculated parameters $G = 5\times10^{6}$ and $N_v' = 1.11\times10^{3}$ into Eq. (18) we obtain

$$F'_{film} = 1.25 \times 10^{-3} \frac{\beta\varepsilon(K - 1)}{1 - KY_b/Y_s} \quad \text{ft-c} \tag{19}$$

The exposure time required to obtain an acceptable film density is given by [16]

$$t \approx \frac{2.25}{F'_{film} \cdot (ASA)} \quad \text{sec} \tag{20}$$

where (ASA) is the film speed. Inserting Eq. (19) into Eq. (20),

$$t = 1.8 \times 10^{3} \frac{1 - KY_b/Y_s}{\beta\varepsilon(K-1)(ASA)} \tag{21}$$

As an example, the exposure time for a high-contrast sample ($Y_s >> 10Y_b$) assuming $\varepsilon = 5\times10^{-3}$, K = 10 and ASA = 400, is t = 100 sec for β = 1 ($P = P_{min}$) and t = 10 sec for β = 10 ($P = 10P_{min}$). The exposure time can also be decreased by increasing ε or the film speed. However, the parameters β, ε, and film speed also affect the image quality as shown in the following argument.

If we assume that individual photoelectron events are detectable, the statistical properties of the image are determined by the total number of electrons emitted from a sample resolution area element r^2_{sys} during a typical exposure. In a time t such an area element emits

$$N = N_s t\, r^2_{sys} \quad \text{electrons} \tag{22}$$

Substituting the derived expressions for t and r_{sys} from Eqs. (21) and (16) and setting $N_s = \beta P_{min} Y_s$, we obtain for this system

$$N = 2 \times 10^{-10} \frac{M^2}{\varepsilon \cdot (ASA)} [1600 + 1.3\times10^{11}/M^2] \text{ electrons} \tag{23}$$

Assuming Poisson statistics apply to the electron emission we may define a signal-to-noise ratio $N/\delta N \approx N/\sqrt{N} = \sqrt{N}$. The result is

$$S/N = 1.4\times10^{-5} \frac{M}{[\varepsilon \cdot (ASA)]^{\frac{1}{2}}} [1600 + 1.3\times10^{11}/M^2]^{\frac{1}{2}} \tag{24}$$

Note that increasing ε or the film speed in order to decrease the exposure time t adversely affects S/N, since a smaller number of electrons are emitted from a resolution element during the exposure. However, S/N is <u>independent</u> of $\beta = P/P_{min}$ since an increase in power input is exactly balanced by a decrease in exposure time, so that the total number of electrons emitted during the exposure remains constant. Thus increasing the incident power is a desirable method of reducing t without sacrificing S/N. Returning to the above example, the S/N for various values of M are:

M	S/N	($\varepsilon = 5\times10^{-3}$; K = 10; ASA = 400)
$\leq$ 1,000	4	
10,000	5	
25,000	10	
50,000	20	

The interesting prediction that S/N will increase with magnification results from the behavior of r^2_{sys} with M. As the magnification is increased, the incident power required to overcome intrinsic noise must increase as M^2 according to Eq. (10). At low M, $r^2_{sys} \propto 1/M^2$ which cancels this factor in the expression for N (Eq. (22)) and S/N is roughly constant. At high M $r_{sys} \approx$ constant and $N \propto M^2$ due to the power requirement term; thus $S/N \propto M$.

A S/N of $\simeq$ 5 is required for distinguishing detail at the resolution limit[18], and thus the predicted values for M $\geq$ 10,000 are quite acceptable. With these operating parameters, some loss of resolution may occur at low magnifications. This is not likely to be a major drawback, since most high-resolution work will be done at M $\geq$ 10,000.

As shown previously, the exposure time t may be reduced from 100 sec at minimum UV power to 10 sec by using $P = 10P_{min}$. In order to bring about a similar change by increasing ε or (ASA), the S/N ratio would decrease by a factor of $\sqrt{10} \approx 3$, which in this case would be unacceptable, especially in the lower range of M. While this sample calculation may not describe exactly a given system, it does point out the compromises involved in obtaining a final image of high quality.

Conclusions

The above calculations specify the conditions needed to proceed with high-resolution photoelectron microscopy of biological surfaces. In order to approach 40 Å lateral resolution a combined instrument and photographic magnification of x50,000 is required. The corresponding minimum UV intensity varies with sample and wavelength, as shown in Tables 2-4. This variation is due to the wavelength dependence of the photoelectron quantum yields, which differs widely among organic and biological samples. Components with higher yields require lower incident intensities to reach a given magnification. For example, the dye phthalocyanine requires between 0.002 and 0.06 Watts/cm^2 for 40 Å resolution imaging against a Formvar substrate. Similar intensities are expected for heme-containing biological samples. A compound like poly-L-tryptophan requires from 0.5 to 10 Watts/cm^2. These intensity values compare favorably with the order of magnitude estimates based on the present limiting magnification and UV intensity of the prototype instrument. The more detailed calculations show explicitly the dependence of incident UV intensity on sample, substrate and microscope parameters.

The total power requirement depends on the type of source used and the UV optical efficiency. In this regard a laser source offers considerable advantages over a conventional arc or discharge lamp. For a tightly focused laser source (A = 100 μ^2), the optical power needed to image proteins against a dark substrate lies in the 10^{-3} - 0.05 milliwatt range. If the beam were defocused by a factor of 10 in area, the total power needed is still less than or on the order of 1 milliwatt. Finally, regardless of the type of source, statistical considerations show that with reasonable film and camera parameters, acceptable signal-to-noise ratios are obtainable throughout the useful magnification range of the instrument.

Acknowledgments

We are indebted to Drs. Gail Massey and Charles A. Burke and also to George H. Lesch for useful discussions. The photoelectron microscopes are funded by PHS Grant no. CA 11695 from the National Cancer Institute. The light source development is funded by NSF grant no. BMS 74-11824. R.J.D. and O.H.G. wish to acknowledge support from grant no. GM 00715-17 and CDA Grant no. 1 K04 CA23359 from the National Cancer Institute, respectively.

References

1. Griffith, O.H., Lesch, G.H., Rempfer, G.F., Birrell, G.B., Burke, C.A., Schlosser, D.W., Mallon, M.H., Lee, G.B., Stafford, R.G., Jost, P.C. and T.B. Marriott. Photoelectron Microscopy: A New Approach to Mapping Organic and Biological Surfaces. Proc. Nat. Acad. Sci. USA 69, 561 (1972).
2. Dam, R.J., Lesch, G.H., Deamer, D.W. and O.H. Griffith. Photoelectron Microscopy of Biomembranes: Observation of External Photoemission from Spinach Chloroplasts. Proc. Electron Microscopy Soc. Amer. 33, 502 (1975).
3. Birrell, G.B., Burke, C.A., Dehlinger, P. and O.H. Griffith. Contrast in the Photoelectric Effect of Organic and Biochemical Surfaces. A First Step Towards Selective Labeling in Photoelectron Microscopy. Biophys. J. 13, 462 (1973).
4. Burke, C.A., Birrell, G.B., Lesch, G.H. and O.H. Griffith. Depth Resolution in Photoelectron Microscopy of Organic Surfaces. The Photoelectric Effect of Phthalocyanine Thin Films. Photochem. Photobiol. 19, 29 (1974).
5. Dam, R.J., Burke, C.A. and O.H. Griffith. Photoelectron Quantum Yields of the Amino Acids. Biophys. J. 14, 467 (1974).
6. Engel, W.and S. Grund. Photoelectron Emission Microscopy of Biological Specimens. Proc. 8th Intl. Congress on Electron Microscopy, Canberra, (1974); Vol. II, p. 656.
7. Dam, R.J., Kongslie, K.F. and O.H. Griffith. The Photoelectron Quantum Yields of Hemin, Hemoglobin and Apohemoglobin: Possible Applications to Photoelectron Microscopy of Heme Proteins in Biological Membranes. Biophys. J. 14, 933 (1974).
8. Dam, R.J., Kongslie, K.F. and O.H. Griffith. Photoelectron Quantum Yields and Photoelectron Microscopy of Chlorophyll and Chlorophyllin. Photochem. Photobiol. 22, 265 (1975).
9. Grund, S., Engel, W. and P. Teufel. Photoelektronen Emissionsmikroskop und

Immunofluoreszenz. J. Ultrastructure Res. 50, 294 (1975).
10. Dam, R.J., Rempfer, G.F. and O.H. Griffith. Photoelectron Microscopy of Organic Surfaces: The Effect of Substrate Reflectivity. J. Appl. Phys., in press (1976).
11. Wegmann, L. The Photo-Emission Electron Microscope. Its Technique and Applications. J. Microscopy 96 (1), 1 (1972).
12. Engel, W. Emission Microscopy with Different Kinds of Electron Emission. Proc. 6th Intl. Congress Electron Microscopy, Kyoto; 217 (1966).
13. Massey, G.A. Efficient Upconversion of Long-Wavelength UV Light into the 200-235 nm Band. Appl. Phys. Lett. 24, 371 (1974).
14. Pong, W. and J.A. Smith, Photoelectric Emission from Copper Phthalocyanine. J. Appl. Phys. 44, 174 (1973).
15. Schechtman, B.H. Photoemission and Optical Studies of Organic Solids: Phthalocyanines and Porphyrins. Technical Report no. 5207-2 from Stanford Electronics Laboratories, Stanford University, Stanford, California (1968).
16. Loveland, R.P. Photomicrography, Vols. I and II, John Wiley & Sons, New York (1970).
17. Klein, M.V. Optics, John Wiley & Sons, New York (1970).
18. Valentine, R.C. The Response of Photographic Emulsions to Electrons, in Advances in Optical and Electron Microscopy, Vol. I, R. Barer and V.E. Cosslett, eds., Academic Press, New York (1968).